



HAL
open science

A unified framework for exponential stability analysis of irrational transfer functions in the parametric space

Rachid Malti, Milan Rapaic, Vukan Turkulov

► To cite this version:

Rachid Malti, Milan Rapaic, Vukan Turkulov. A unified framework for exponential stability analysis of irrational transfer functions in the parametric space. 2022. hal-03646956v2

HAL Id: hal-03646956

<https://hal.science/hal-03646956v2>

Preprint submitted on 28 Sep 2022 (v2), last revised 17 Jan 2024 (v4)

HAL is a multi-disciplinary open access archive for the deposit and dissemination of scientific research documents, whether they are published or not. The documents may come from teaching and research institutions in France or abroad, or from public or private research centers.

L'archive ouverte pluridisciplinaire **HAL**, est destinée au dépôt et à la diffusion de documents scientifiques de niveau recherche, publiés ou non, émanant des établissements d'enseignement et de recherche français ou étrangers, des laboratoires publics ou privés.

A unified framework for exponential stability analysis of linear irrational systems in the parametric space [★]

Rachid Malti ^a, Milan R. Rapaic ^b, Vukan Turkulov ^b

^a*Univ. Bordeaux, IMS – UMR 5218 CNRS, France*

^b*Faculty of Technical Sciences, Trg Dositeja Obradovića 6, University of Novi Sad, Serbia*

Abstract

This paper presents a unified framework for exponential stability analysis of linear stationary systems with irrational transfer functions in the space of an arbitrary number of unknown parameters. Systems described by irrational transfer functions may be of infinite dimension, typically having an infinite number of poles and/or zeros, rendering their stability analysis more challenging as compared to their finite-dimensional counterparts. The analysis covers distributed parameter systems, time delayed systems of both retarded and neutral type, or even fractional systems. First, it is proven that, under mild hypotheses, new poles may appear to the right of a vertical axis of abscissa γ (when $\gamma = 0$: imaginary axis) through a continuous variation of parameters only if existing poles to the left of γ cross the vertical axis. Hence, by determining parametric values for which the crossing occurs, known as stability crossing sets (SCS), the entire parametric space is separated into regions within which the number of right-half poles (including multiplicities) is invariant. Based on the aforementioned result, a robust estimation algorithm is formulated as an interval constraint satisfaction problem and solved using guaranteed methods, for determining the SCS. The developed algorithm is applied for assessing stability of (i) a controlled parabolic 1D partial differential equation, namely the heat equation, in finite and semi-infinite media, (ii) time-delay rational systems with distributed and retarded type delays, (iii) fractional systems, providing stability results even for incommensurate differentiation orders.

Key words: Stability; Time-delay systems; Distributed parameter systems; Irrational transfer systems; Interval arithmetics

1 Introduction

Many engineering systems exhibit dynamical behaviors that can be captured by partial differential equations (PDE), or delayed ordinary (and partial) differential equations. These distributed parameter systems (DPS) yield irrational transfer functions that are usually infinite dimensional, with an infinite number of poles and/or zeros. A wide variety of transfer functions of DPS, solutions of PDE, is exhibited in (Curtain & Morris, 2009).

This paper presents stability analysis of irrational transfer functions in the parametric space. Similar methods have been investigated for stability analysis of time-delay-systems (TDS) in (Gryazina, 2004; Neimark, 1998; Lee & Hsu, 1969; El'sgol'ts & Norkin, 1973). They split the parametric space into multiple regions, with the

number of unstable poles being invariant inside each region. An alternative approach consists of finding the stability crossing sets (SCS), i.e. a set of surfaces for which there is at least a pole crossing the imaginary axis. Such approaches have been successfully demonstrated for retarded systems with two and three independent delays (Hale & Huang, 1993; Gu, Niculescu & Chen, 2005; Sipahi & Delice, 2009; Gu & Naghnaeian, 2011), providing insightful graphical representation of stability equivalence regions. To the best of authors' knowledge, such methods have never been extended to other types of irrational transfer functions.

A new method, based on the application of Rouché's theorem from complex analysis (see e.g. (Lang, 1999)), in the frequency domain, has recently been proposed for stability analysis of fractional order systems (FoS) in (Rapaic & Malti, 2019) and a large class of retarded and distributed TDS in (Turkulov, Rapaic & Malti, 2022). Given a parametrized FoS and/or TDS and an arbitrary parametric point, the proposed method identifies the surrounding region in the parametric space for which the number of unstable poles remains invariant.

[★] This paper was not presented at any IFAC meeting. Corresponding author R. Malti

Email addresses: rachid.malti@ims-bordeaux.fr (Rachid Malti), rapaja@uns.ac.rs (Milan R. Rapaic), vukan_turkulov@uns.ac.rs (Vukan Turkulov).

Nyquist stability criterion is another important tool that has been continuously used for stability analysis of irrational transfer functions of (i) DPS in (Chait, MacCluer & Radcliffe, 1989; Logemann, 1991), (ii) time-delay FoS in (Zhang, Liu & Xue, 2020), and (iii) incommensurate FoS in (Ivanova, Moreau & Malti, 2016). Some other well-known finite-dimensional results, such as circle criterion and small gain theorem, have been generalized to a large class of DPS in (Logemann, 1991).

Another class of methods is based on the state-space representation and some special forms of Lyapunov–Krasovskii functionals. It is used to derive simple finite dimensional conditions in terms of LMI’s for assessing stability of distributed parameter systems with time delays in (Fridman & Orlov, 2009), and of uncertain fractional order systems of neutral type with distributed delays in (Aghayan, Alfi & Machado, 2021). Additionally, direct Lyapunov method is used in (Katz & Fridman, 2020) for guaranteeing stability of a finite dimensional observer based control of a 1-D parabolic PDE (linear heat equation). Similarly, Prieur & Trélat (2019) synthesize stabilizing boundary control subject to a constant delay for a reaction-diffusion partial differential equation by stabilizing unstable poles of infinite dimensional systems.

Several methods are developed for analyzing stability of more specific DPS such as clamped-free damped string (Lhachemi, Saussié, Zhu & Shorten, 2020), telegrapher’s equation (Sano, 2018), heat equation (Li, Zhou & Gao, 2018; Li & Gao, 2021), wave equation (Gao, Ma & Sun, 2019; Ha-Duong & Joly, 1994).

A unified framework is proposed in this paper for exponential stability analysis of linear stationary systems in the frequency domain explicitly presented in a transfer function form. The proposed method is based on computing the SCS and applies to a wide range of transfer functions (Curtain & Morris, 2009) that are (i) solutions of some partial differential equations, with or without delays, under some boundary conditions, which may include terms like $e^{-\sqrt{s}}$, $\cosh(\sqrt{s})$, or $\sinh(\sqrt{s})$, of the Laplace variable s , (ii) TDS with retarded, incommensurate or distributed delays, (iii) FoS, with or without time-delays, which may have incommensurate differentiation orders and which stability analysis is more challenging than the commensurate ones.

The paper is organized as follows. Notation and hypotheses are presented in the next section followed by the problem formulation. Then, theoretical results regarding pole continuity are presented in section 2, followed by a robust estimation algorithm of the SCS, based on interval arithmetics, in section 3. Applications to DPS, TDS, and FoS are presented in sections 4, 5, and 6 respectively, before concluding.

1.1 Notation

The paper utilizes standard mathematical notations. The set of non-negative and non-positive real numbers are respectively denoted by \mathbb{R}^+ and \mathbb{R}^- . \mathbb{C} is the field of complex numbers, \mathbb{C}_γ^+ and $\overline{\mathbb{C}_\gamma^+}$ are respectively the sets of all complex numbers with real part bigger than γ , and bigger or equal to γ . Consequently, \mathbb{C}_0^+ and $\overline{\mathbb{C}_0^+}$ denote respectively the open and the closed right-half complex planes.

Stability. Consider several subalgebras of transfer functions, as discussed in (Curtain & Zwart, 1995; Partington & Bonnet, 2004). A transfer function G is said to be stable in the \mathcal{H}_∞ sense if it is holomorphic and bounded in \mathbb{C}_0^+ . Next, consider the class $\hat{\mathcal{A}}_\beta$ as the class of all transfer functions that are holomorphic in $\Re(s) > -\beta$ and continuous on the boundary $\Re(s) = -\beta$, with finite and unique limit when $s \rightarrow -\beta \pm j\infty$. For $\beta > 0$, $\hat{\mathcal{A}}_\beta$ is referred to as the subalgebra of β -exponentially stable transfer functions. On the other hand, a transfer function belonging to $\hat{\mathcal{A}}_\beta$ for some negative β , but not for any $\beta \geq 0$, is referred to as exponentially unstable. Note that for $\beta_2 > \beta_1 > 0$, $\hat{\mathcal{A}}_{\beta_2} \subset \hat{\mathcal{A}}_{\beta_1} \subset \hat{\mathcal{A}}_0 \subset \mathcal{H}_\infty$.

Characteristic function and stability crossing sets. When dealing with linear time-invariant (LTI) rational systems, the concept of a characteristic polynomial is well defined as transfer function denominator. It allows assessing system stability by studying the root locus of the characteristic polynomial, since they are the only singularities of the transfer function.

When dealing with LTI, irrational systems denoted $G(s, \boldsymbol{\theta})$, where $s \in \mathbb{C}$ is the Laplace variable, and $\boldsymbol{\theta} = (\theta_1, \dots, \theta_n) \in \mathcal{T} \subset \mathbb{R}^n$ is the parametric vector, the concept of characteristic function (instead of polynomial) $f(s, \boldsymbol{\theta})$ requires some clarifications. In the present work, the characteristic function is understood as any function $f(s, \boldsymbol{\theta})$ such that for every $\boldsymbol{\theta} \in \mathcal{T}$

- (1) f has no finite poles of any multiplicity,
- (2) f has branch points and/or essential singularities everywhere G has branch points and/or essential singularities¹,
- (3) all finite zeros of f match poles of G in both location and multiplicity.

The selection of the characteristic function is not unique. Several different characteristic functions may be constructed from a single transfer function, according to the points above. For example, a characteristic function of

¹ The distinction between different types of singularities is made on the basis of the shape of the Laurent series, as studied in complex analysis (see e.g. (Lang, 1999))

a given transfer function $G(s, \boldsymbol{\theta})$ could be derived as

$$f(s, \boldsymbol{\theta}) = \frac{Q(s, \boldsymbol{\theta})}{G(s, \boldsymbol{\theta})}, \quad (1)$$

with Q being an analytic function in \mathbb{C} having zeros, with matching multiplicities, at the same locations as the zeros of G . Without loss of generality, transfer functions with poles-zeros cancellations are not handled in this paper. If such cases occur, they should be treated separately.

Additionally, let $\Omega_{f, \gamma}$ denote the *stability crossing set* (SCS) of f , i.e. a set of surfaces for which there is at least a zero of f crossing the axis $\Re(s) = \gamma$

$$\Omega_{f, \gamma} = \{\boldsymbol{\theta} \in \mathcal{T} \mid (\exists \omega \in \mathbb{R}) f(\gamma + j\omega, \boldsymbol{\theta}) = 0\}. \quad (2)$$

Let $NU_{f, \gamma}(\boldsymbol{\theta})$ denote the number of zeros of a characteristic function $f(s, \boldsymbol{\theta})$ with real part bigger or equal to γ , where each zero is counted as many times as its multiplicity. Although multiple characteristic functions may be defined for an irrational transfer function, the stability crossing sets are well-defined and independent of the selection of f .

1.2 Problem formulation

Consider an LTI system with transfer function $G(s, \boldsymbol{\theta})$ and characteristic equation $f(s, \boldsymbol{\theta})$, $\boldsymbol{\theta} \in \mathcal{T} \subset \mathbb{R}^n$ (with \mathcal{T} being the parametric space). Choose $\gamma \in \mathbb{R}$ such that $G(s, \boldsymbol{\theta})$ has finite and unique limit for $s \rightarrow \gamma \pm j\infty$, all singularities of f have real parts smaller or equal to γ , with Ξ denoting the set of imaginary parts of all singularities of f on the axis $\Re(s) = \gamma$. The problem under consideration is partitioning the parametric space into non-overlapping sub-regions \mathcal{T}_k ($k \in 1, \dots, K$) such that for all k

- i) $f(s, \boldsymbol{\theta})$ has no zero on the axis $\Re(s) = \gamma$, for all $\boldsymbol{\theta} \in \mathcal{T}_k$, and
- ii) $NU_{f, \gamma}(\boldsymbol{\theta}_1) = NU_{f, \gamma}(\boldsymbol{\theta}_2)$ for all $\boldsymbol{\theta}_1, \boldsymbol{\theta}_2 \in \mathcal{T}_k$.

Formally, the following hypotheses are postulated:

- (H1) For every $\boldsymbol{\theta} \in \mathcal{T}$, $s \mapsto f(s, \boldsymbol{\theta})$ is analytic in $\overline{\mathbb{C}_\gamma^+}$ ², except possibly in a finite set of points on the boundary, $\gamma + j\omega$ for $\omega \in \Xi = \{\omega_1, \dots, \omega_N\}$. For every $(s, \boldsymbol{\theta}) \in (\overline{\mathbb{C}_\gamma^+} \setminus (\gamma + j\Xi)) \times \mathcal{T}$, $(s, \boldsymbol{\theta}) \mapsto f(s, \boldsymbol{\theta})$ is continuous.

² A function is analytic in a closed set if and only if it is analytic in every point of that set. For sets having nonempty boundary (like $\overline{\mathbb{C}_\gamma^+}$) this actually means that the function is also analytic in some (possibly small) neighborhood of that boundary. In other words, a function analytic in a closed set is also analytic in some open superset that encloses that set.

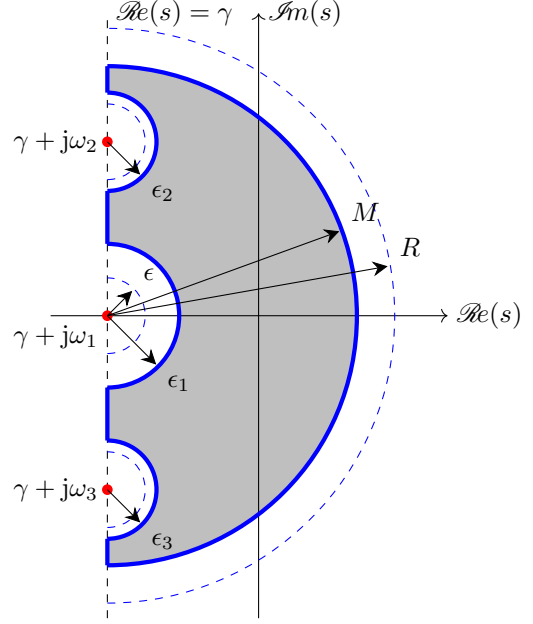


Fig. 1. Illustration of the notation involved in the hypotheses (H1)-(H3) and in the proof of Theorem 2.

- (H2) For all $\gamma + j\omega_k$, $\omega_k \in \Xi$, there exists $\epsilon_k > 0$ such that $f(s, \boldsymbol{\theta}) \neq 0$ for all s satisfying $\Re(s) \geq \gamma$ and $|s - \gamma - j\omega| \leq \epsilon_k$, and all $\boldsymbol{\theta} \in \mathcal{T}$.
- (H3) There exists $M > 0$ such that $f(s, \boldsymbol{\theta}) \neq 0$ for all $\boldsymbol{\theta} \in \mathcal{T}$ and all s such that $\Re(s) \geq \gamma$ and $|s - \gamma| \geq M$.

Hypothesis (H1) serves two purposes. Firstly, it ensures that the transfer function is parameterized in a continuous fashion with respect to s and $\boldsymbol{\theta}$, except possibly at a finite number of points on $\Re(s) = \gamma$. Those singular points, illustrated by red dots in Fig.1, are gathered within the set $j\Xi$. Secondly, (H1) determines the type of guaranteed stability one is able to seek for. If (H1) is satisfied for some $\gamma < 0$, then it is possible to investigate for exponential stability, by localizing zeros of the characteristic function. If it is satisfied for some $\gamma \geq 0$, but not for any smaller γ , then the system under consideration is exponentially unstable, regardless of the position of the zeros of f . However, if (H1) is satisfied for $\gamma \geq 0$, but not for any smaller γ , then neither exponential stability nor exponential instability can be claimed solely based on the position of roots of the characteristic equation. In this case, stability should be investigated by additional considerations, e.g. \mathcal{H}_∞ -stability can be claimed by establishing that the transfer function is bounded on $\overline{\mathbb{C}_0^+}$ (Partington & Bonnet, 2004).

The introduced hypotheses also limit the extent of the parametric space \mathcal{T} . Hypothesis (H2) is a safeguard from cases in which zeros of the characteristic function in $\overline{\mathbb{C}_\gamma^+}$ either originate from or terminate at the singularities located on the imaginary axis. A simple example would be a system with characteristic function $f(s, K) = K + s^{-\frac{3}{2}}$,

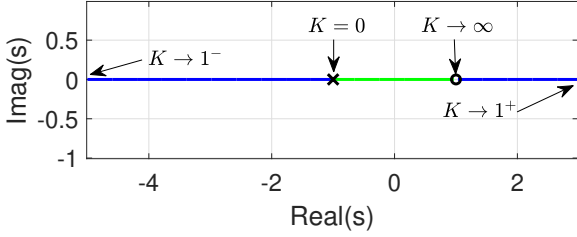


Fig. 2. Root locus of closed loop system with loop transfer function $L(s, K) = K \frac{1-s}{1+s}$.

having a zero with positive real part originating from the branch point at the origin when $K < 0$. This however is not permitted by (H2) which hence restricts the study of $f(s, K)$ to $K > 0$. Hypothesis (H3) guards against cases in which zeros emerge from infinity in \mathbb{C}_γ^+ . It, for example, prevents negative values of delays (non-causal leads), and also safeguards against cases in which system structure abruptly changes for certain parametric values. An interesting practical example is the case of loop transfer function with relative degree zero, such as e.g. $L(s, K) = K \frac{1-s}{s+1}$, which closed-loop characteristic polynomial is $f(s, K) = (s+1) - K(s-1)$. In this particular case, a single branch of the root locus originates at $s = -1$ for $K = 0$. By increasing K the root slides along the negative real axis, and reaches asymptotically $-\infty$ when $K \rightarrow 1^-$, as illustrated in Fig.2. The value $K = 1$ is singular, since the order of the system changes, and for this particular value of K the characteristic polynomial has no zero. However when $K > 1$, a root pops up from $+\infty$, and decreases asymptotically to $s = 1$ as K grows. Consequently, the characteristic function of this system does not fulfill hypothesis (H3) when $K \in \mathbb{R}$. However, it is worth mentioning that (H3) allows investigating separately the stability for $0 \leq K < 1$.

Within the present work and under hypothesis (H1)-(H3), we start by proving that the only way for the number of zeros of a characteristic function to change in \mathbb{C}_γ^+ , when the parameters vary continuously, is by crossing the vertical axis $\Re(s) = \gamma$. This theoretical result, related to root continuity, is studied in section 2. Then, the problem of finding the SCS is formulated as a constraint satisfaction problem in section 3 and a robust estimation algorithm, based on interval arithmetics, is detailed to solve it. Unlike many previously published results, mainly focused on time-delay systems (TDS) (Hale & Huang, 1993; Gu et al., 2005; Sipahi & Delice, 2009; Gu & Naghnaeian, 2011), a unified framework is proposed in the present paper that applies to a large variety of irrational systems, regardless of the number of investigated parameters. The only practical limitation is related to the exponential complexity of the proposed algorithm.

2 Root Continuity

The following claims will ensure continuity of all right-half zeros of the characteristic function. Start by recalling the root continuity result from (Dieudonné, 1960, Theorem 9.17.4).

Theorem 1 *Let D be an open set in \mathbb{C} , \mathcal{T} a metric space, f a continuous, complex valued function in $\mathbb{C} \times \mathcal{T}$ such that for each $\theta \in \mathcal{T}$ $s \mapsto f(s, \theta)$ is analytic in D . Let D_1 be an open subset of D whose closure $\overline{D_1}$ is compact and contained in D , and let θ_0 be such that no zero of $f(s, \theta_0)$ is on the boundary of D_1 . Then, there exists a neighborhood W of θ_0 such that for every $\theta \in W$*

- (1) *there are no zeros of $f(s, \theta)$ on the boundary of D_1 , and*
- (2) *the sum of the orders of zeros of $f(s, \theta)$ belonging to D_1 is independent of θ .*

Dieudonné's Theorem, formulated on a compact set, was previously used, in (Cooke & Grossman, 1982; Gu et al., 2005), for stability analysis of TDS, by investigating the SCS. Unlike TDS, irrational transfer functions may have branch points and essential singularities on the imaginary axis (see e.g. sections 4 and 6) and more generally on the axis $\Re(s) = \gamma$. Hence, an extension of theorem 1 is required taking into account the non-compact set $\overline{\mathbb{C}_\gamma^+} \setminus (\gamma + j\Xi)$ that has a finite number of singularities on the boundary $\Re(s) = \gamma$. In fact, hypotheses (H1)-(H3) are introduced precisely to enable this extension, formulated in the following.

Theorem 2 *Under hypotheses (H1)-(H3), given any connected subset \mathcal{S} of \mathcal{T} , if $f(\gamma + j\omega, \theta) \neq 0$ for all $\omega \in \mathbb{R} \setminus \Xi$ and all $\theta \in \mathcal{S}$, then for any $\theta_1, \theta_2 \in \mathcal{S}$ the number of zeros of f in $\overline{\mathbb{C}_\gamma^+}$, counting multiplicities, is the same: $NU_f(\theta_1) = NU_f(\theta_2)$.*

PROOF. According to (H1), there exists an open set D containing $\overline{\mathbb{C}_\gamma^+} \setminus (\gamma + j\Xi)$ such that f is continuous on $D \times \mathcal{T}$. Let M satisfy (H3), and select an arbitrary $R \geq \max\{M, |\omega_1|, \dots, |\omega_N|\}$, with $\omega_k \in \Xi$. Consider ϵ_k , introduced in (H2), and define $0 < \epsilon \leq \min_k \epsilon_k$. Introduce set $\overline{D_1}$ as the closed set bounded by the axis $\Re(s) = \gamma$ excluding $\gamma + j[\omega_k - \epsilon, \omega_k + \epsilon]$, "small" semi-circles $\gamma + j\omega + \epsilon^{j\varphi}$ and the "big" semi-circle $\gamma + Re^{j\varphi}$ (with $\varphi \in [-\frac{\pi}{2}, \frac{\pi}{2}]$). Let D_1 be the interior of $\overline{D_1}$. Due to hypotheses (H2), (H3), and the condition $f(\gamma + j\omega, \theta) \neq 0$ assumed in the statement of the Theorem, there can be no zeros of f on the boundary of D_1 for all $\theta \in \mathcal{S}$. Therefore, D_1 satisfies all the assumptions of Theorem 1. Consequently, for all $\theta_0 \in \mathcal{S}$ there exists a neighborhood $W(\theta_0) \subset \mathcal{S}$ such that the number of zeros of f inside D_1 , including multiplicities, is independent of $\theta \in W(\theta_0)$.

Notice further that this implies that the number of zeros (including multiplicities) of f is constant within $\overline{\mathbb{C}_\gamma^+}$, since due to (H2) there can be no right-half singularities within the “small” semicircles of D_1 , and due to (H3) there can be no roots in \mathbb{C}_γ^+ with modulus greater than $M < R$. Consequently, for every $\theta_0 \in \mathcal{S}$ there exists a neighborhood $W(\theta_0)$ such that the number of zeros in $\overline{\mathbb{C}_\gamma^+}$ is independent of $\theta \in W(\theta_0)$. In the remainder, it is proven by contradiction that the number of zeros of f with real part bigger or equal to γ , including multiplicities, does not change within the entire set \mathcal{S} . Assume that the number of roots, counting multiplicities, is not the same for every $\theta \in \mathcal{S}$. Then, there exists at least two parametric points $\theta_1, \theta_2 \in \mathcal{S}$ such that the number of zeros at θ_1 is different from the one at θ_2 . Since \mathcal{S} is connected by assumption, there exists a simple path $\mathcal{P} \subset \mathcal{S}$ connecting θ_1 and θ_2 , and at least one point $\theta_0 \in \mathcal{P}$ such that the number of zeros, counting multiplicities, is not constant in any neighborhood of θ_0 , which contradicts the existence of $W(\theta_0)$ and completes the proof. \square

Definition 3 Given a parametric space \mathcal{T} , and an LTI system with characteristic function $f(s, \theta)$ with stability crossing set $\Omega_{f, \gamma}$, defined in (2), any two points θ_1 and θ_2 from \mathcal{T} are said to belong to the same **parametric region** if there exists a continuous path within \mathcal{T} connecting θ_1 with θ_2 which does not intersect $\Omega_{f, \gamma}$.

Notice that “belong to the same parametric region” is an equivalence relation. Therefore, the stability crossing set splits the parametric space \mathcal{T} into multiple disjoint regions \mathcal{T}_k , $k = 1, \dots, K \leq \infty$ such that

$$\mathcal{T} = \Omega_{f, \gamma} \cup \bigcup_{k=1, \dots, K} \mathcal{T}_k.$$

An immediate consequence of Theorem 2 is that given any parametric region \mathcal{T}_k of \mathcal{T} , and any pair of points $\theta_1, \theta_2 \in \mathcal{T}_k$, the number of zeros in $\overline{\mathbb{C}_\gamma^+}$, counting multiplicities, is the same for $f(s, \theta_1)$ and $f(s, \theta_2)$. Thus, under hypotheses (H1)-(H3), zeros of the characteristic function cannot suddenly appear or change multiplicity in $\overline{\mathbb{C}_\gamma^+}$. The only way for the number of zeros to change is by crossing the axis $\Re(s) = \gamma$ when system parameters vary continuously. Hence, the determination of the SCS, $\Omega_{f, \gamma}$ defined in (2), allows characterizing all the regions in the parametric space inside which the characteristic function has the same number of zeros.

The required theoretical results for root continuity being established, the problem of finding the SCS is formulated and solved in the next section.

3 Robust estimation algorithm of the SCS

Since the parameters gathered in θ vary continuously, the problem of determining stability regions can be re-

sumed to the problem of finding the SCS, defined in (2), for which the zeros of $f(s, \theta)$ cross the imaginary axis. This problem is formulated as a Constraint Satisfaction Problem (CSP):

$$\text{CSP: } \begin{cases} f(\gamma + j\omega, \theta) = 0 \\ (\omega, \theta) \in \{\mathbb{R}^+ \setminus \Xi\} \times \mathcal{T} \end{cases} \quad (3)$$

The searching space is restricted to $\{\mathbb{R}^+ \setminus \Xi\}$, because all real-valued impulse-response systems have complex conjugate poles. The solution set of all the feasible parameters of the CSP (3) is rewritten as

$$\mathbb{S} = \left\{ (\omega, \theta) \in \{\mathbb{R}^+ \setminus \Xi\} \times \mathcal{T} \mid f(\gamma + j\omega, \theta) = 0 \right\}. \quad (4)$$

A guaranteed and robust solution of this CSP can be obtained, in the searching domain, using interval arithmetics introduced by (Moore, 1966). The reader is also referred to (Jaulin, Kieffer, Didrit & Walter, 2001) for an introduction to interval arithmetics. The characterization of the whole solution set \mathbb{S} in (4) can be formulated as a set inversion problem

$$\mathbb{S} = f^{-1}(0) \cap \{\mathbb{R}^+ \setminus \Xi\} \times \mathcal{T} \quad (5)$$

and solved by guaranteed methods based on contraction and bisection.

3.1 Contractors

Let $[x] = [\underline{x}, \bar{x}]$ design an interval which is a closed, bounded, and connected set of real numbers. The CSP (3) can be solved by a contractor \mathcal{C} , which is an operator which permits to reduce the domain $[\zeta] = ([\omega], [\theta])$ without any bisection. Hence, contracting the box $[\zeta]$ means replacing it by a smaller box $[\zeta]^*$ such that the solution set \mathbb{S} remains unchanged, i.e. $\mathbb{S} \subset [\zeta]^* \subset [\zeta]$. There exists different types of contractors depending on whether the system to be solved is linear or not (Jaulin et al., 2001).

3.2 Set Inversion Via Interval Analysis (SIVIA)

The SIVIA algorithm (Jaulin & Walter, 1993) has been proposed to solve constraint propagation problems using bisection. It has been used in different contexts such as: state and parameter estimation of non linear systems (Raïssi, Ramdani & Candau, 2004), robust estimation of frequency domain models (Khemane, Malti, Raïssi & Moreau, 2012), parameter estimation in a glucose model (Herrero, Delaunay, Jaulin, Georgiou, Oliver & Toumazou, 2016), or even to compute invariant sets of closed-loop control systems (Romig, Jaulin & Rauh, 2019).

Applying the SIVIA algorithm to (3) allows obtaining

```

1: procedure SIVIA(in:  $[t]$ ,  $[\zeta]$ ,  $\eta$ ,  $\bar{\mathbb{S}}$ ; out:  $\bar{\mathbb{S}}$ )
2:   option: call contractor (in:  $[\zeta]$ ; out:  $[\zeta]$ )
3:   if  $[t]([\zeta]) = [0]$  then return;
4:   end if
5:   if  $w([\zeta]) \leq \eta$  then
6:      $\bar{\mathbb{S}} := \bar{\mathbb{S}} \cup [\zeta]$ ;
7:     return;
8:   else
9:     bisect  $[\zeta]$  into  $[\zeta_1]$  and  $[\zeta_2]$ ;
10:     $\bar{\mathbb{S}} = \text{SIVIA}([t], [\zeta_1], \eta, \bar{\mathbb{S}})$ 
11:     $\bar{\mathbb{S}} = \text{SIVIA}([t], [\zeta_2], \eta, \bar{\mathbb{S}})$ 
12:    return;
13:   end if
14: end procedure

```

Algorithm 1. SIVIA algorithm with only an outer enclosure

an outer enclosure $\bar{\mathbb{S}}$ of the solution set \mathbb{S} , if it exists³ as defined in (4), such that $\mathbb{S} \subseteq \bar{\mathbb{S}}$. SIVIA is a recursive algorithm based on partitioning of the parameter set into three regions: feasible, indeterminate and unfeasible. However, only indeterminate and unfeasible regions³ can be obtained for the \mathcal{CSP} (3). Hence the presentation of the SIVIA algorithm is restrained to these two cases. It uses an inclusion test $[t] : \{\mathbb{R}^+ \setminus \Xi\} \times \mathcal{T} \rightarrow \mathbb{N}$ which is a function allowing to prove if a box $[\zeta]$ is unfeasible or undetermined. If unfeasible, the box is simply ignored. If undetermined, it is bisected and tested again unless its width $w([\zeta])$ is less than a precision parameter η tuned by the user and which ensures that the algorithm terminates after a finite number of iterations. The outer enclosure $\bar{\mathbb{S}}$ is then computed as a union of all undetermined boxes as indicated in line 6 of Algorithm 1. Line 2 allows calling optionally a contractor at each execution of the SIVIA algorithm.

In this paper, the SIVIA algorithm guarantees that all the outer enclosures of the SCS are obtained in the desired searching box which should be chosen carefully together with the precision factor η due to the exponential complexity of the algorithm. Hence, the more prior knowledge is introduced regarding the position of the SCS, the better. When no prior knowledge is available, the SIVIA algorithm may be initialized with a large searching box and a big precision factor η in such a way to obtain a rough estimation of the SCS. Then, the searching box can be narrowed and the precision factor enhanced to get more precise outer enclosures.

The SIVIA algorithm is implemented using INTLAB toolbox (Rump, 1999) in different contexts: a controlled heat equation in section 4, rational TDSs in section 5, and FoS in section 6.

³ The original SIVIA algorithm allows computing additionally an inner enclosures: $\underline{\mathbb{S}} \subseteq \mathbb{S} \subseteq \bar{\mathbb{S}}$. However, the \mathcal{CSP} formulated in (3), can only yield an outer enclosure $\bar{\mathbb{S}}$.

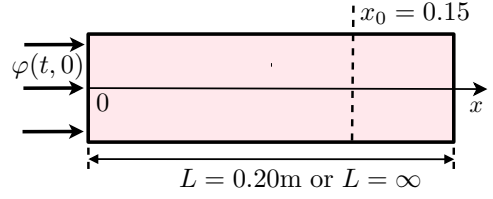


Fig. 3. Thin rod of length L .

4 Application to stability analysis of a distributed parameter system

Consider a one-dimensional heat diffusion in a thin rod⁴ of length $0 < L \leq \infty$. The rod is thermally isolated, except at its boundary cross-sections as in Fig.3. At the initial end $x = 0$, the rod is subject to an adjustable thermal flux, $\varphi(t, 0) = -\lambda \frac{\partial \theta}{\partial x}(t, 0)$, where λ is the thermal conductivity. Two cases are treated: either the rod is of finite length or infinite. When the rod length is finite, the opposite end is kept at ambient temperature $\theta(t, L) = 0$. The corresponding model describing spatio-temporal distribution of the temperature along the rod is given by the well-known *heat equation*,

$$\frac{\partial^2 \theta(t, x)}{\partial x^2} = \sigma^{-1} \frac{\partial \theta(t, x)}{\partial t}, \quad (6)$$

where σ is the thermal diffusivity of the medium. The temperature of the rod is measured at a cross-section $x = x_0 = 0.15\text{m}$, with $0 \leq x_0 \leq L$. This temperature is then controlled remotely (see Fig.4) using a proportional controller with a gain K . Additionally, time required to transmit data from the controller to the actuator, and from the sensor to the controller is denoted by $\frac{\tau}{2}$, so that the total loop delay is $\tau \geq 0$. Hence, the effective transfer function of the proportional delayed controller is

$$P(s) = K e^{-\tau s} \quad (7)$$

The objective of this example is to find the whole set of stabilizing controllers (7) in the K versus τ plane in both cases: finite and semi-infinite rods. A similar problem is treated in (Morărescu & Niculescu, 2007), with the same delayed proportional controller $P(s)$, however applied to a rational system.

4.1 Semi-infinite spatial domain ($L = \infty$)

In the semi-infinite domain, the transfer function between the input flux $\Phi(s, 0) = \mathcal{L}\{\varphi(t, 0)\}$ and the temperature $\Theta(s, x) = \mathcal{L}\{\theta(t, x)\}$ at a cross-section x is

⁴ For numerical application, the rod is considered of aluminium type with a thermal diffusivity $\sigma = 98.8 \times 10^{-6} \text{ m}^2/\text{s}$ and a conductivity $\lambda = 237 \text{ Wm}^{-1}\text{K}^{-1}$ (see e.g. (Baehr & K., 2011)).

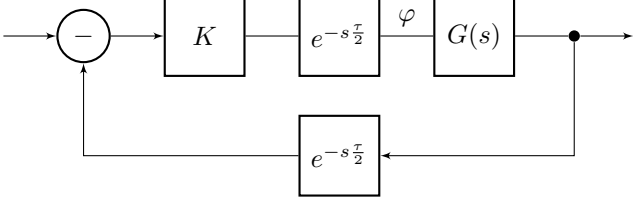


Fig. 4. A feedback control loop, where $G(s)$ is the transfer function between the heat flux and the temperature at x_0 , for either a semi-infinite or a finite rod, $P(s)$ is a proportional delayed controller as in (7).

(Curtain & Morris, 2009)

$$G(s) = \frac{\Theta(s, x)}{\Phi(s, 0)} = \frac{e^{-x\sqrt{\frac{s}{\sigma}}}}{\lambda\sqrt{\frac{s}{\sigma}}}, \quad (8)$$

with the closed-loop transfer function $\frac{Ke^{-s\tau}e^{-x\sqrt{\frac{s}{\sigma}}}}{f(s, K, \tau)}$ and the closed-loop characteristic function

$$f(s, K, \tau) = \lambda\sqrt{\frac{s}{\sigma}} + Ke^{-s\tau}e^{-x\sqrt{\frac{s}{\sigma}}}. \quad (9)$$

Due to the presence of \sqrt{s} a branch-cut is necessary. It is chosen along the negative real axis including the branch point 0 and ∞ . Hence, the characteristic function $f(s, K, \tau)$ is holomorphic in the complement of the branch-cut line of the complex plane and the arguments of s are restrained to

$$|\arg(s)| < \pi \quad (10)$$

Due to the presence of a branch point at the origin, the proposed algorithm is applied with $\gamma = 0$.

In the special case when $\tau = 0$, all the roots of $f(s, K, 0)$ can be determined analytically and their locus plotted versus K . The solutions of $f(s, K, 0) = 0$ are given by all the determinations, $n = 0, \pm 1, \pm 2, \dots$, of Lambert's W_n function, see e.g. (Corless, Gonnet, Hare, Jeffrey & Knuth, 1996), $s = \frac{\sigma}{x^2} W_n^2\left(-\frac{Kx}{\lambda}\right)$, provided (10) is fulfilled. The root locus of $f(s, K, 0)$ is plotted versus gain K , in Fig.5, for the principal determination of the Lambert function W_0 (as the upper imaginary part) and for the determination W_{-1} (as the lower imaginary part). The other determinations of $W_n, n = 1, \pm 2, \pm 3, \dots$ are not represented as they are well beyond the scale of Fig.5 towards $-\infty$. They may yield other poles crossing the imaginary axis for values of K that are much greater than the ones represented in Fig.5, which shows that two poles pop up from the branch-cut when $K \approx 3 \times 10^3$. They cross the imaginary axis towards instability when $K \approx 56 \times 10^3$. The objective of the paper is to determine for what parametric values (here K and in a more general case K and τ) the poles cross the imaginary axis.

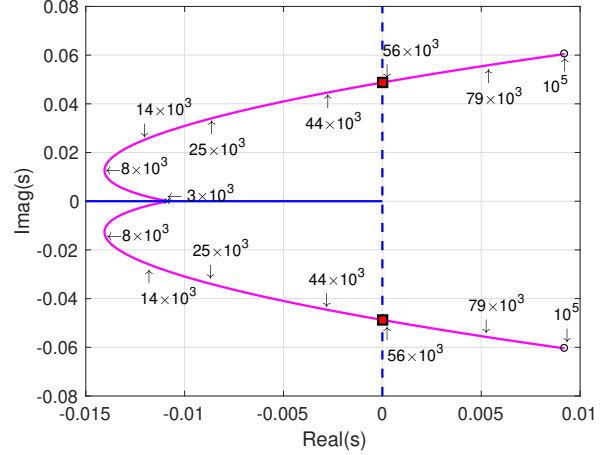


Fig. 5. Root locus of $f(s, K, 0)$ in (9) for different values of K , illustrating that poles pop up from the plane-cut. When the poles cross the imaginary axis (red squares), the system becomes unstable. Numbers on the curves correspond to values of K . The plane-cut is represented in blue along \mathbb{R}^- .

4.2 Finite spatial domain ($L < \infty$)

In this case, the following transfer function is obtained for the heat diffusion process under consideration (Curtain & Morris, 2009)

$$G(s) = \frac{\Theta(s, x)}{\Phi(0, s)} = \frac{\sinh((L-x)\sqrt{\frac{s}{\sigma}})}{\lambda\sqrt{\frac{s}{\sigma}} \cosh(L\sqrt{\frac{s}{\sigma}})}, \quad (11)$$

with the closed loop characteristic function

$$f(s, K, \tau) = \lambda\sqrt{\frac{s}{\sigma}} \cosh\left(L\sqrt{\frac{s}{\sigma}}\right) + Ke^{-s\tau} \sinh\left((L-x)\sqrt{\frac{s}{\sigma}}\right). \quad (12)$$

As in the previous example, the proposed algorithm is applied with $\gamma = 0$, due to the presence of a branch point at the origin.

4.3 Robust estimation algorithm of the SCS

Both characteristic functions (9) and (12) comply with the hypotheses (H1)-(H3). They have a branch point at $s = 0$, which is excluded from the searching box ($\Xi = \{0\}$), initialized at

$$[\zeta] = ([\omega], [K], [\tau]) = ([10^{-3}, 0.1], [0, 7 \cdot 10^4], [0, 100]) \quad (13)$$

Although theoretically the searching interval of ω is $\mathbb{R}^+ \setminus \{0\}$, the thermal system under consideration is slow. Additionally, one can see from Fig.5 that the root locus of (9) for $\tau = 0$ crosses the imaginary axis for an ω in the interval (0.04, 0.05). Consequently, the first poles crossing the imaginary axis towards instability, in both cases

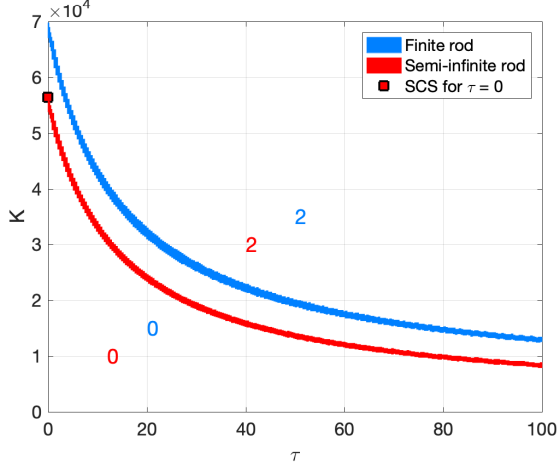


Fig. 6. Outer enclosures of the SCS in the finite and semi-infinite aluminium rods. The number of unstable poles is indicated inside each region (by the corresponding color). The red square corresponds to the SCS of $f(s, K, 0)$ in (9) as predicted in the root locus of Fig.5 (red square).

(9) for any τ and (12), are expected to be within the frequency interval $[10^{-3}, 0.1]$ rad/sec. In case the obtained outer enclosure of $[\omega]$ touches either the lower bound 10^{-3} or the upper bound 0.1, the searching interval is enlarged and the SIVIA algorithm run again. The tolerance is set to an arbitrarily small value as the width of each element $w([\zeta])$ divided by 2^8

$$\eta = w([\zeta])/2^8 \quad (14)$$

$$\eta = (0.39 \cdot 10^{-3}, 273.4, 0.39) \quad (15)$$

The obtained outer enclosures of the stability crossing sets are plotted in the K versus τ plane in Fig.6 in red for the semi-infinite rod and in blue for the finite rod. The position of the poles crossing the imaginary axis is plotted, with the same colors, in Fig.7. Since both transfer functions (8) and (11) are bounded on the imaginary axis, the systems under consideration are \mathcal{H}_∞ -stable in the parametric regions for which there are no roots in $\overline{\mathbb{C}_0^+}$ (the lower left parts of Fig. 6). Hence, the red line (similarly the blue) in Fig.6 splits the plane into two regions: a guaranteed stability region (the lower left containing $K = 0$ and $\tau = 0$) and a guaranteed instability region as the upper right one. In between, the outer enclosures of the SCS are plotted. Their width can be reduced by reducing the precision factor η in (14) at the price of a higher computational burden. In the case of the semi-infinite rod, for $\tau = 0$, the results of Figs.6 and 7 (red squares) are confirmed by the intersection of the root-locus with the imaginary axis, in Fig.5.

To the best of authors' knowledge, in both cases finite with $\tau \neq 0$ and semi-infinite aluminium rods, there is no analytical method allowing to compute the roots of the characteristic function f in (9) or (12). The only

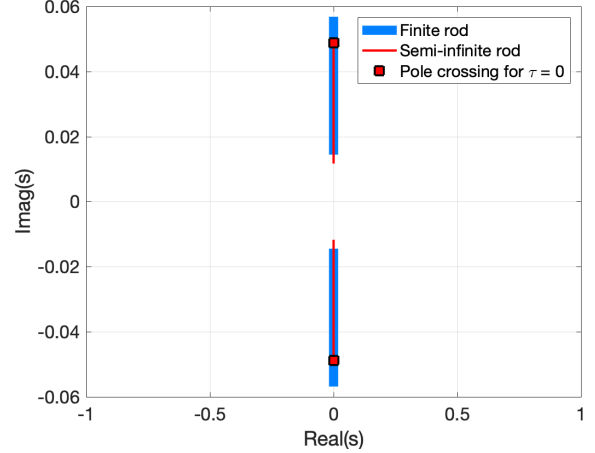


Fig. 7. Outer enclosures of the frequencies crossing the imaginary axis in the finite and semi-infinite aluminium rods. The red squares correspond to the pole crossing of $f(s, K, 0)$ in (9) as predicted in the root locus of Fig.5 (red square).

alternative method for evaluating exponential stability of the control loop is based on a graphical representation that uses Cauchy's principle argument.

5 Application to stability analysis of time delay systems

5.1 Distributed delay system

Consider in this section a distributed delay system taken from (Turkulov et al., 2022, example 9) modeled by

$$\dot{x}(t) = - \int_{-\tau}^0 e^{K\alpha} x(t + \alpha) d\alpha. \quad (16)$$

Its characteristic function, computed by straightforward integration of the Laplace transform of (16),

$$f(s, K, \tau) = s^2 + sK + 1 - e^{-\tau(s+K)}, \quad (17)$$

complies with the hypotheses (H1)-(H3), with no singularities in $\overline{\mathbb{C}_\gamma^+}$. Hence the boundary of instability region is investigated by choosing $\gamma = 0$ and $\gamma = -0.02$. The searching box is initialized at

$$[\zeta] = ([\omega], [K], [\tau]) = ([0, 1.5], [0, 0.3], [0, 20]), \quad (18)$$

and the tolerance factor set as in (14). The obtained outer enclosures of the SCS are plotted in the K versus τ plane in Fig.8, which confirms and extends the results of (Turkulov et al., 2022, example 8) obtained using Rouché's theorem. The exterior of the blue curve corresponds to systems of class $\mathcal{A}_{0,0.2}$. The outer enclosures of $[\omega]$, for which the poles cross respectively the imaginary axis $\Re(s) = 0$ and the axis $\Re(s) = -0.02$ are $[0.31, 1.42]$ and $[0.31, 1.56]$.

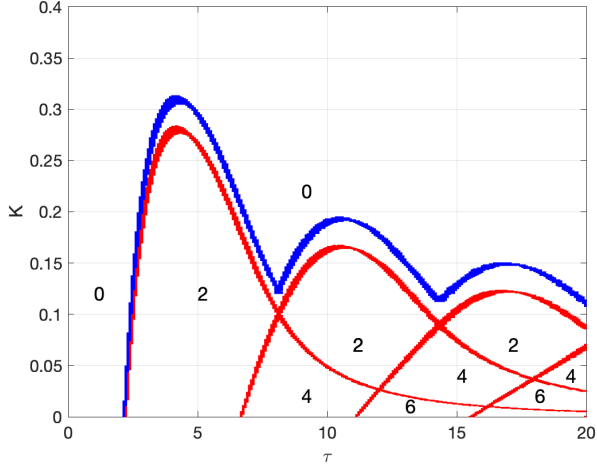


Fig. 8. Outer enclosures of the SCS of $f(s, K, \tau)$ in (17) in red for $\gamma = 0$ and in blue for $\gamma = -0.02$ (only the external part is sketched in the latter case); the number of unstable poles is indicated inside each region. Outside the blue region, the system is guaranteed to belong to $\mathcal{A}_{0.02}$.

5.2 Time delay system of retarded-type

Consider a TDS system of retarded type, taken from (Turkulov et al., 2022, example 10), with a characteristic function given by

$$f(s, \tau_1, \tau_2) = s^2 + 2se^{-s\tau_1} + e^{-s\tau_2}. \quad (19)$$

Its stability is investigated with respect to τ_1 and τ_2 by setting the initial searching box to

$$[\zeta] = ([\omega], [\tau_1], [\tau_2]) = ([0.45, 2.5], [0, 1.8], [0, 3]). \quad (20)$$

The obtained outer enclosures of the SCS are plotted in the τ_1 versus τ_2 plane in Fig.9. The number of unstable poles, computed at any point inside the different regions, is indicated by a number. Fig.9 confirms again and extends the results of (Turkulov et al., 2022, example 10) obtained using Rouché's theorem. The interior of the blue contour indicates the region of the parametric space corresponding to systems of class $\mathcal{A}_{0.02}$. The obtained outer enclosure of $[\omega]$ for which the poles cross the imaginary axis is $[0.48, 2.42]$.

6 Application to stability analysis of a fractional system

Consider in this section a fractional system, taken from (Rapaic & Malti, 2019, example 3), with a characteristic function given by

$$f(s, \alpha_1, \alpha_2) = s^{\alpha_2} + 2s^{\alpha_1} + 1 \quad (21)$$

and $(\alpha_1, \alpha_2) \in \{\mathbb{R}^+ \setminus \{0\}\}^2$. When α_1 and/or α_2 are non integers, the characteristic function $f(s, \alpha_1, \alpha_2)$ is

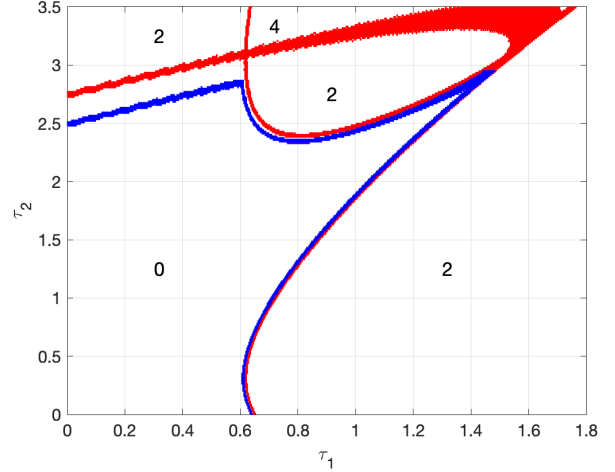


Fig. 9. Outer enclosures of the the SCS of $f(s, \tau_1, \tau_2)$ in (19) in red for $\gamma = 0$ and in blue for $\gamma = -0.02$ (only the internal part is sketched in the latter case); the number of unstable poles is indicated inside each region. Inside the blue region, the system is guaranteed to belong to $\mathcal{A}_{0.02}$.

holomorphic in the complement of the branch-cut line of the complex plane. The branch-cut is chosen to be along the negative real axis including the branch point at 0 and ∞ , and the restriction (10) applies to s .

The proposed algorithm is applied for determining the SCS of $f(s, \alpha_1, \alpha_2)$ with $\gamma = 0$. The characteristic function (21) complies with the hypotheses (H1)-(H3). The branch point at $s = 0$ is excluded from the searching box ($\Xi = \{0\}$), initialized at:

$$[\zeta] = ([\omega], [\alpha_1], [\alpha_2]) = ([0.1, 4], [0.1, 15], [0.1, 20]) \quad (22)$$

with a tolerance set arbitrarily to a small value as in (14). The obtained outer enclosures \bar{S} of the SCS, is plotted in Fig.10 which confirms the results of (Rapaic & Malti, 2019, example 3). The outer enclosure of $[\omega]$ for which the poles cross the imaginary axis is $[0.56, 1.79]$. Hence, all fractional systems, incommensurate and commensurate, that have differentiation orders in the lower-left region of Fig.10, have no unstable poles. Considering additionally that $G(s) = f^{-1}(s, \alpha_1, \alpha_2)$ is bounded on \mathbb{C}_0^+ , one may also conclude that the parametric region with $NU_{f,0} = 0$ is the region of \mathcal{H}_∞ -stability.

7 Conclusions

A unified framework has been presented in this paper for exponential stability analysis of irrational transfer functions in the frequency domain. First, it has been proven that the only way for the number of zeros of a characteristic function to change in the right of a vertical axis of abscissa γ , when its parameters vary continuously, is by crossing that vertical axis. Based on this theoretical

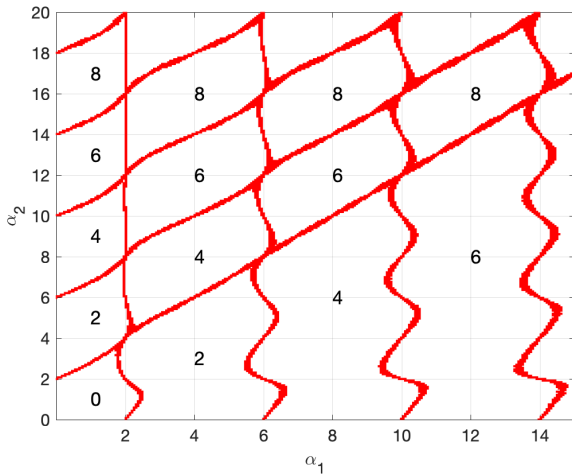


Fig. 10. Outer enclosures of the SCS of $f(s, \alpha_1, \alpha_2)$ in (21). The number of unstable poles is indicated inside each region.

result, the problem of finding the set of parameters for which poles cross the vertical axis has been formulated as a constraint satisfaction problem. This original formulation is universal as it applies to a wide class of irrational transfer functions. It has been solved using the robust SIVIA algorithm, based on interval arithmetics, that uses contraction and bisection. It has been successfully applied for determining the SCS of (i) a controlled heat partial differential equation, in finite and semi-infinite media, (ii) time-delay systems with distributed and retarded type delays, (iii) fractional systems, providing stability results even for incommensurate differentiation orders. The proposed algorithm may be used for any number of transfer function parameters. The only limitation is related to the time-complexity of the SIVIA algorithm which is known to be exponential in terms of the number of parameters. Hence, the more prior knowledge can be introduced for initializing the searching box, the better. The examples presented in the paper have been intentionally limited to two parameters for graphical representation purposes.

References

- Aghayan, Z. S., Alfi, A., & Machado, J. T. (2021). Robust stability of uncertain fractional order systems of neutral type with distributed delays and control input saturation. *ISA Transactions*, *111*, 144–155.
- Baehr, H. D. & K., S. (2011). *Heat and Mass Transfer* (3rd ed.). Springer.
- Chait, Y., MacCluer, C., & Radcliffe, C. (1989). A nyquist stability criterion for distributed parameter systems. *IEEE Transactions on Automatic Control*, *34*(1), 90–92.
- Cooke, K. L. & Grossman, Z. (1982). Discrete delay, distributed delay and stability switches. *Journal of Mathematical Analysis and Applications*, *86*(2), 592–627.
- Corless, R. M., Gonnet, G. H., Hare, D. E. G., Jeffrey, D. J., & Knuth, D. E. (1996). On the lambertw function. *Advances in Computational Mathematics*, *5*(1), 329–359.
- Curtain, R. & Morris, K. (2009). Transfer functions of distributed parameter systems: A tutorial. *Automatica*, *45*(5), 1101–1116.
- Curtain, R. F. & Zwart, H. (1995). *An Introduction to Infinite-Dimensional Linear Systems Theory*. New York, NY: Springer New York.
- Dieudonné, J. (1960). *Foundations of Modern Analysis*. Academic Process, NY and London.
- El’sgol’ts, L. E. & Norkin, S. B. (1973). *Introduction to the Theory and Application of Differential Equations with Deviating Arguments*. Academic Press, Inc. (London) LTD.
- Fridman, E. & Orlov, Y. (2009). Exponential stability of linear distributed parameter systems with time-varying delays. *Automatica*, *45*(1), 194–201.
- Gao, R., Ma, N., & Sun, G. (2019). Stability of solution for uncertain wave equation. *Applied Mathematics and Computation*, *356*, 469–478.
- Gryazina, E. (2004). The D-decomposition theory. *Automation and Remote Control*, *65*, 1872–1884.
- Gu, K. & Naghnaeian, M. (2011). Stability crossing set for systems with three delays. *IEEE Transactions on Automatic Control*, *56*(1), 11–26.
- Gu, K., Niculescu, S.-I., & Chen, J. (2005). On stability crossing curves for general systems with two delays. *Journal of Mathematical Analysis and Applications*, *311*(1), 231–253.
- Ha-Duong, T. & Joly, P. (1994). On the stability analysis of boundary conditions for the wave equation by energy methods. part i: The homogeneous case. *Mathematics of Computation - Math. Comput.*, *62*, 539–563.
- Hale, J. & Huang, W. (1993). Global geometry of the stable regions for two delay differential equations. *Journal of Mathematical Analysis and Applications*, *178*(2), 344–362.
- Herrero, P., Delaunay, B., Jaulin, L., Georgiou, P., Oliver, N., & Toumazou, C. (2016). Robust set-membership parameter estimation of the glucose minimal model. *Int. J. of adaptive control and signal processing*, *30*(2), 173–185.
- Ivanova, E., Moreau, X., & Malti, R. (2016). Stability and resonance conditions of second-order fractional systems. *Journal of Vibration and Control*, 1–15.
- Jaulin, L., Kieffer, M., Didrit, O., & Walter, E. (2001). *Applied interval analysis*. London: Springer-Verlag.
- Jaulin, L. & Walter, E. (1993). Set inversion via interval analysis for nonlinear bounded-error estimation. *Automatica*, *29*(4), 1053–1064.
- Katz, R. & Fridman, E. (2020). Constructive method for finite-dimensional observer-based control of 1-d parabolic pdes. *Automatica*, *122*, 109285.
- Khemane, F., Malti, R., Raissi, T., & Moreau, X. (2012). Robust estimation of fractional models in the frequency domain using set membership methods. *Signal Processing*, *92*, 1591–1601.

- Lang, S. (1999). *Graduate texts in Mathematics – Complex Analysis* (4th ed.). USA: Springer, NY.
- Lee, M. S. & Hsu, C. S. (1969). On the tau-decomposition method of stability analysis for retarded dynamical systems. *SIAM Journal on Control*, 7(2), 242–259.
- Lhachemi, H., Saussié, D., Zhu, G., & Shorten, R. (2020). Input-to-state stability of a clamped-free damped string in the presence of distributed and boundary disturbances. *IEEE Transactions on Automatic Control*, 65(3), 1248–1255.
- Li, L. & Gao, H. (2021). The stability and stabilization of heat equation in non-cylindrical domain. *Journal of Mathematical Analysis and Applications*, 493(2), 124538.
- Li, L., Zhou, X., & Gao, H. (2018). The stability and exponential stabilization of the heat equation with memory. *Journal of Mathematical Analysis and Applications*, 466(1), 199–214.
- Logemann, H. (1991). Circle criteria, small-gain conditions and internal stability for infinite-dimensional systems. *Automatica*, 27(4), 677–690.
- Moore, R. (1966). *Interval analysis*. Englewood Cliffs, NJ: Prentice-Hall.
- Morărescu, C.-I. & Niculescu, S. (2007). Stability crossing curves of SISO systems controlled by delayed output feedback. *Dynamics of Continuous, Discrete and Impulsive Systems Series B: Applications & Algorithms*, 14, 659–678.
- Neimark, Y. I. (1998). D-partition and robust stability. *Computational Mathematics and Modeling*, 9(2), 160–166.
- Partington, J. R. & Bonnet, C. (2004). H_∞ and bibo stabilization of delay systems of neutral type. *Systems & Control Letters*, 52(3), 283–288.
- Prieur, C. & Trélat, E. (2019). Feedback stabilization of a 1-d linear reaction–diffusion equation with delay boundary control. *IEEE Transactions on Automatic Control*, 64(4), 1415–1425.
- Raissi, T., Ramdani, N., & Candau, Y. (2004). Set membership state and parameter estimation for systems described by nonlinear differential equations. *Automatica*, 40(10), 1771–1777.
- Rapaić, M. R. & Malti, R. (2019). On stability regions of fractional systems in the space of perturbed orders. *IET Control Theory & Applications*, 13.
- Romig, S., Jaulin, L., & Rauh, A. (2019). Using interval analysis to compute the invariant set of a nonlinear closed-loop control system. *Algorithms*, 12(12).
- Rump, S. (1999). *Developments in reliable computing*, chapter IntLab – Interval laboratory, (pp. 77–104). Kluwer academic publisher.
- Sano, H. (2018). Stability analysis of the telegrapher’s equations with dynamic boundary condition. *Systems & Control Letters*, 111, 34–39.
- Sipahi, R. & Delice, I. I. (2009). Extraction of 3D stability switching hypersurfaces of a time delay system with multiple fixed delays. *Automatica*, 45(6), 1449 – 1454.
- Turkulov, V., Rapaić, M. R., & Malti, R. (2022). Stability analysis of time-delay systems in the parametric space. *Automatica*. Provisionally accepted (see also <https://arxiv.org/abs/2103.15629>).
- Zhang, S., Liu, L., & Xue, D. (2020). Nyquist-based stability analysis of non-commensurate fractional-order delay systems. *Applied Mathematics and Computation*, 377, 125111.